Supplemental Information includes:

- Supplemental Figures and Legends S1 to S5

- Supplemental Experimental Procedures

- Supplemental References

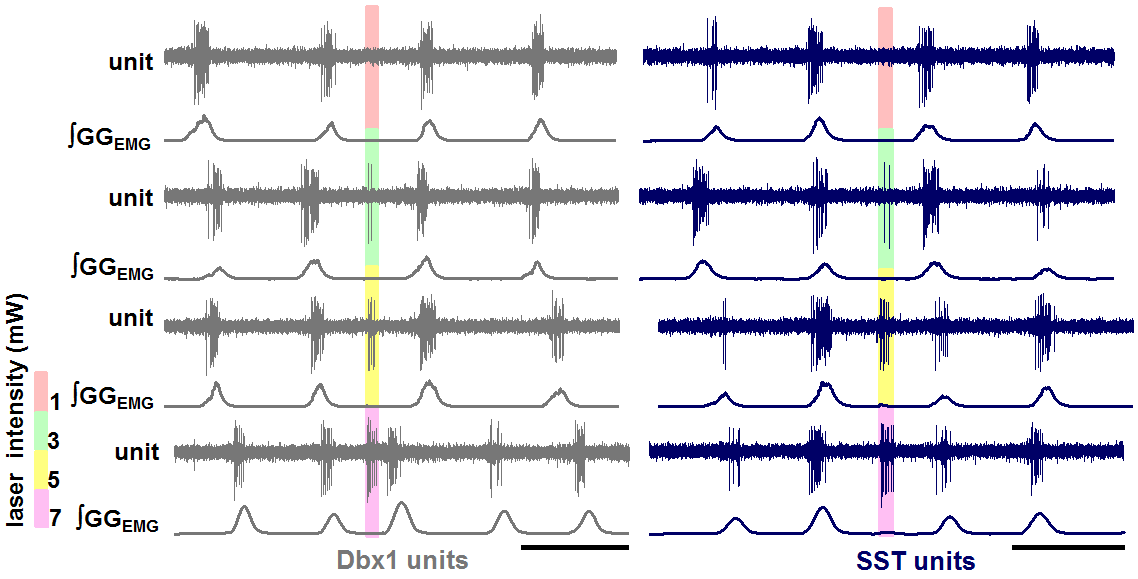

Figure S1, **Related to Figure 2,** Photostimulation of preBötC respiratory-modulated light responsive units in Dbx1-ChR2 (gray) and SST-ChR2 (blue) mice at 4 different laser intensities (red, 1 mW; green, 3 mW; yellow, 5 mW; purple, 7 mW). Scale bar, 1 s.

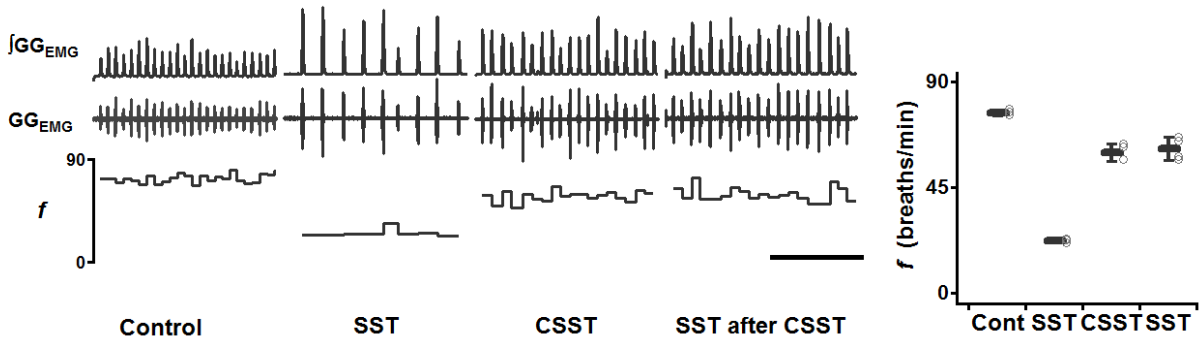

Figure S2, Related to Figure 4A, SST receptors in preBötC effectively blocked by CSST microinjections. Left: GG_{EMG} and $\int GG_{EMG}$ traces show the changes in *f* under the following conditions in anesthetized mice: control; SST: after bilateral injection of SST into preBötC; CSST: after bilateral injection of CSST into preBötC; SST after CSST: after the second bilateral injection of SST , i.e., same dose of SST that resulted in the lower frequency before CSST did not suppress breathing after CSST. Scale bar, 10 s. Right: Breathing frequency (n=4) under the above-described conditions. Error bars represent mean ±SD.

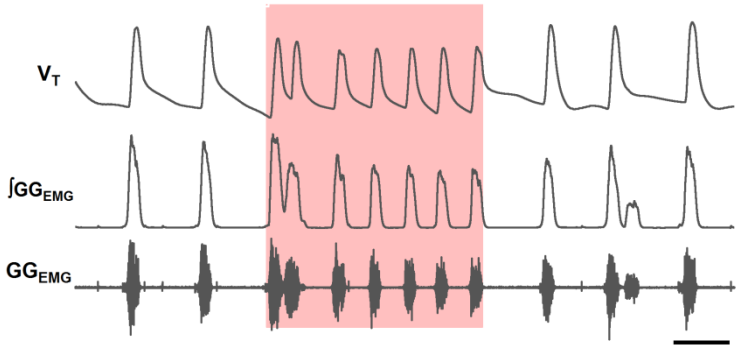

Figure S3, **Related to Figure 6D,** Doublets elicited by bilateral preBötC LPP after block of postsynaptic inhibition in Dbx1-ChR2 mice. Scale bar, 2 s.

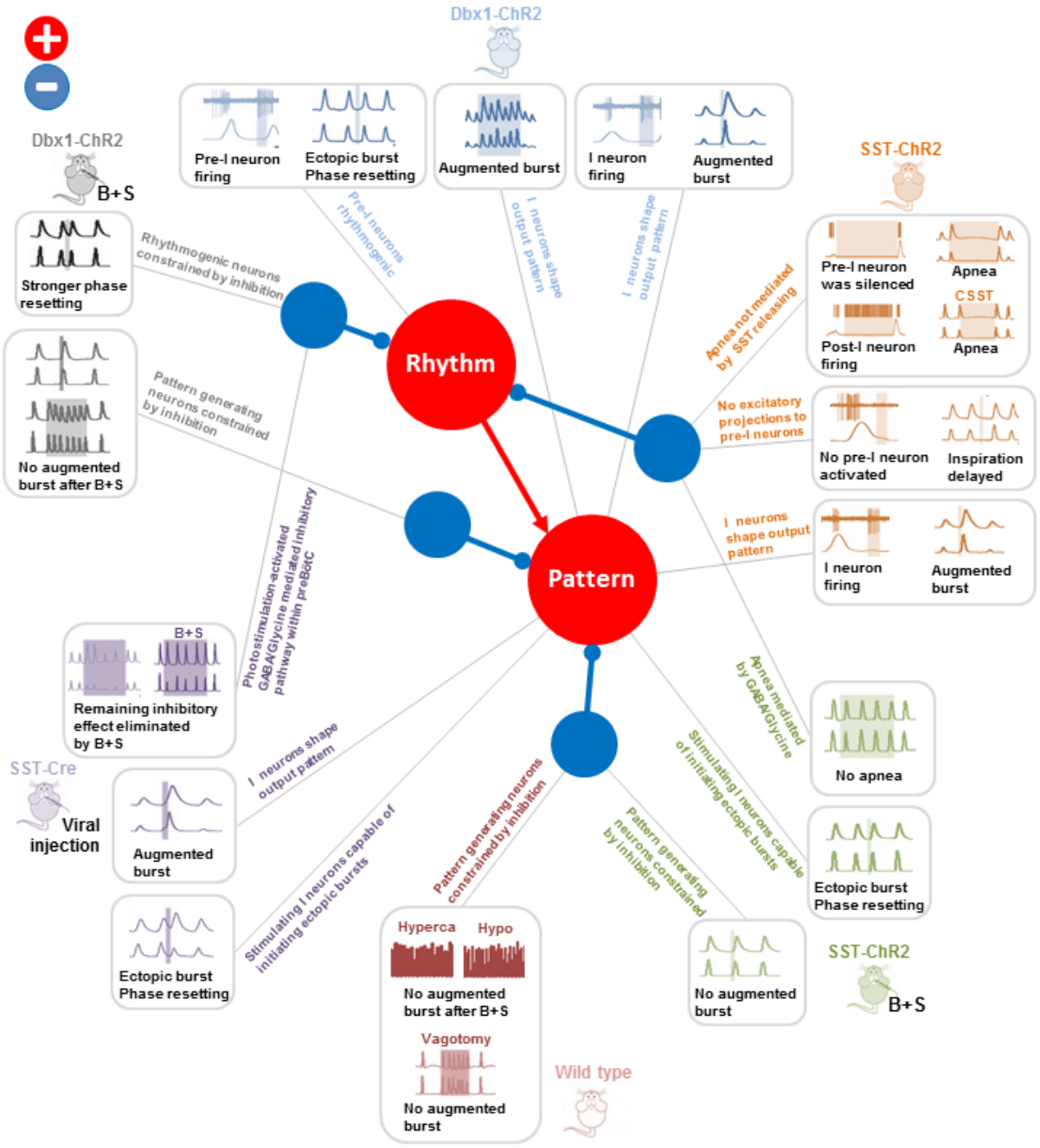

Figure S4, Related to Figure 8, Parceling effects of photoactivating preBötC respiratory-related neuronal subpopulations in mice on breathing. The core excitatory circuit of rhythmogenic preinspiratory neurons exciting pattern generating inspiratory neurons (red circles) is modulated by various inhibitory subpopulations (blue circles). The gray lines represent our interpretation of the site(s) of various effects of photostimulation (in rounded rectangles) in different mouse models, i.e., directly on rhythm or pattern generating preBötC circuits (red) or via inhibitory neurons (blue), either within or outside preBötC.

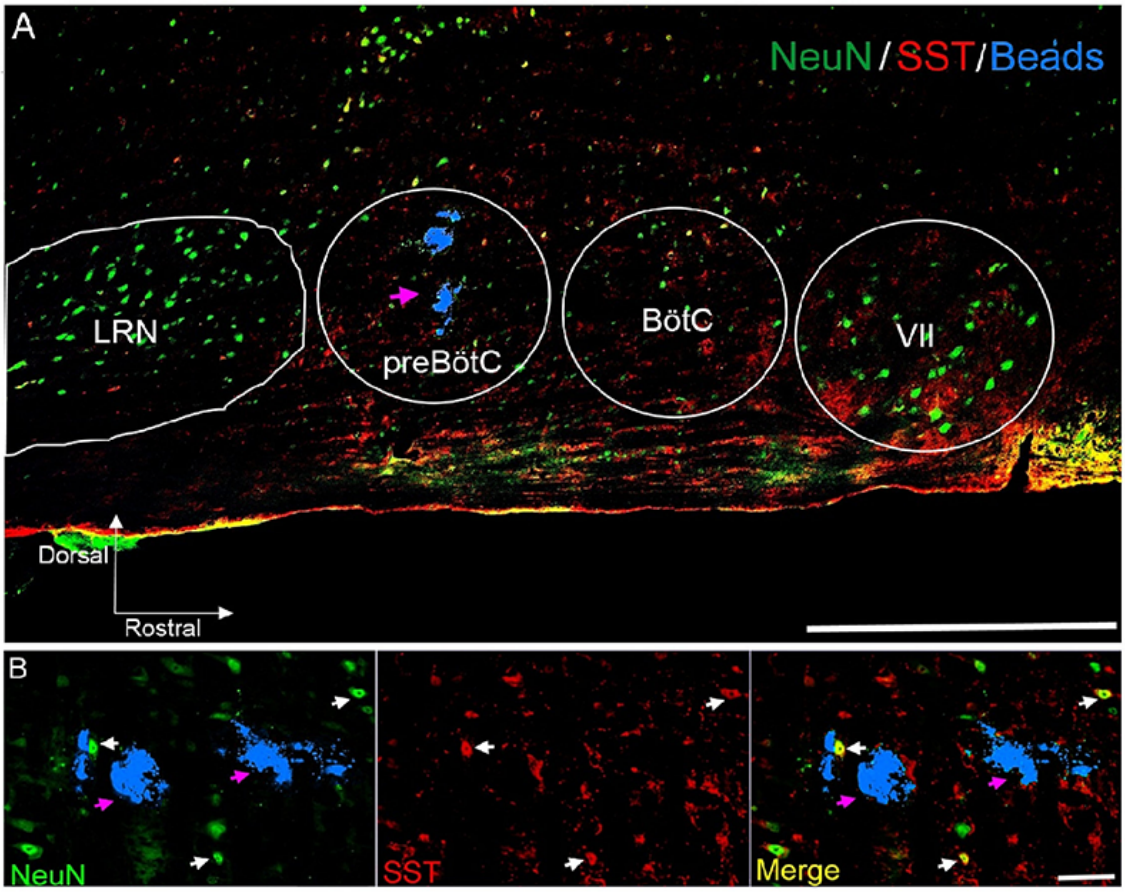

Figure S5, Related to the Experimental Procedures, Example of injection site in preBötC for bicuculline/strychnine or CSST demarked by coinjection of florescent beads. A, Representative confocal mosaic micrograph of sagittal brainstem section shows the location of preBötC injection of bicuculline and strychnine (purple arrow). Scale bar, 500 μm. VII, facial nucleus; BötC, Bötzinger Complex; LRN, lateral reticular nucleus. B, High-magnification micrograph showing fluorescent beads (purple arrows) intermingled with SST^+ neurons (white arrows). Scale bar, 50 μm.

Supplemental Experimental Procedures

Animals

Transgenic mice were generated by crossing mice expressing Cre recombinase either in Dbx1-derived neurons (Dbx1-Cre mice: Dbx1-Cre animals were a gift from J. Corbin, Bielle et al., 2005), or SST^{+} neurons (Sst-IRES-Cre, abbreviated as SST-Cre: *Sst*$^{tm2.1(cre)Zjh}$/J, Stock Number: 013044, obtained from Jackson labs), with *floxed-ChR2-tdTomato* mice (Ai27; ChR2(H134R)-tdTomato; Jackson labs, Stock Number: 012567). These crosses generated mice expressing ChR2 in either Dbx1-derived neurons (Dbx1-Cre;ChR2(H134R)-tdTomato, abbreviated as Dbx1-ChR2) or SST^{+} neurons (Sst-IRES-Cre;ChR2(H134R)-tdTomato, abbreviated as SST-ChR2). Viral injections were performed on adult male SST-Cre mice (Jackson labs, Stock Number: 013044). All experiments in this study were performed on adult male mice, either wild type (24-28 g) or SST-Cre (26-30 g; average post-surgery duration of ~30 days), Dbx1-ChR2 (28-36 g), or SST-ChR2 (24-30 g). Unless otherwise specified, mice were vagus intact.

Viral vector design

We used an adeno-associated viruses (AAV2) encoding ChR2-eYFP driven by the constitutive promoter Ef1α in a double floxed inverted open reading frame configuration (DIO-ChR2). The viral construct *AAV2/1-Ef1α-DIO-ChR2-eYFP* (Addgene plasmid 20298; provided by K. Deisseroth, Stanford University, Palo Alto, CA; Cardin et al., 2009) was produced by the University of Pennsylvania Gene Therapy Program Vector Core. We used a ChR2 variant with the H134R mutation, which produces a twofold increase in the steady-state current as compared to the wild type variant of ChR2 (Adamantidis et al., 2007; Gradinaru et al., 2007).

Viral injections

Mice were anesthetized with isoflurane (4% for induction and 2% for maintenance) and placed in a stereotaxic apparatus (David Kopf Instruments) with Bregma and Lambda skull landmarks level. Two holes were drilled in the skull 6.80 mm caudal to Bregma and 1.2 mm lateral to the midline (Paxinos and Franklin, 2003). 100-200 nl of virus solution (ChR2: 5-10x10^{12} GC/ml) per side was then injected 4.65 mm ventral from the dorsal surface of the brain into the preBötC through a glass pipette connected to a pressure ejection system (Picospritzer II; Parker Hannafin). The pipette was left in place for 5 min after injection to minimize backflow. The wound was closed with 5-0 non-absorbable sutures. The mice were returned to their home cage and given 2-3 weeks to recover to allow for sufficient levels of protein to express.

Surgical procedures for ventral approach

Adult mice were anesthetized with ketamine and xylazine (100 and 10 mg/kg, respectively, i.p.). Atropine (0.5 mg/kg, i.p.) was given to prevent bradycardia and excessive airway secretion. Isoflurane (1-2% volume in air) was administered throughout an experiment. The level of anesthesia was assessed by the suppression of the withdrawal reflex. A tracheostomy tube was placed in the trachea through the larynx, and respiratory flow was detected with a flow head connected to a transducer to measure airflow (GM Instruments) that was integrated for tidal volume (V_T). Coupled EMG wire electrodes (Cooner Wire) were inserted into the genioglossus (GG) muscles. Wires were connected to amplifiers (Grass Model P511; Grass Instruments) and activity was sampled at 2-4 kHz (Powerlab 16SP; AD Instruments). The mice were placed in a supine position in a stereotaxic instrument (David Kopf Instruments). The larynx was denervated, separated from the pharynx, and moved aside. The basal aspect of the occipital bone was removed to expose the ventral aspect of the medulla. The canal of the hypoglossal nerve (XII) served as a suitable landmark. The preBötC were 0.15 mm caudal to the hypoglossal canal, 1.2 mm lateral to the midline, and 0.24 mm dorsal to the ventral medullary surface.

Photostimulation

Once the ventral brainstem surface was exposed, a 473 nm laser (OptoDuet Laser; IkeCool) connected to a branching fiber patch cord with two 200 µm diameter fibers (Doric Lenses) was placed in soft contact with the ventral surface, 0.15 mm caudal to the hypoglossal canal and 1.2 mm lateral to the midline (Figure 1E), ~250 µm ventral to the preBötC. Laser power was set at 7 mW. Short Pulse Photostimulation (SPP; 100-300 ms) and Long Pulse Photostimulation (LPP; 4-10 s) were delivered under the command of a pulse generator (Pulsemaster A300 Generator; WPI) connected to the laser power supply. Stimulating ventral neuronal axons in the midline, or 600 µm rostral/caudal to preBötC in Dbx1-ChR2 or SST-ChR2 mice served as a control and did not produce significant effects. No effects were produced by preBötC photostimulation 10 s after bilateral preBötC lesion in Dbx1-ChR2 mice.

Pharmacological injection experiments

Bicuculline methiodide (Tocris Bioscience), a $GABA_A$ receptor antagonist, and strychnine hydrochloride (Sigma-Aldrich), a glycine receptor antagonist, were injected together (B+S, 250 µM each, 50-60 nl/side) to block fast inhibitory synaptic transmission. Cyclosomatostatin (125 µM, 50-60 nl/side; Sigma-Aldrich) was used as a broad spectrum somatostatin receptor antagonist. Fluorescent polystyrene beads (0.2% solution; Invitrogen) diluted in saline were injected for post hoc confirmation of injection sites (Figure S5, purple arrow), and somatostatin (SST) immunoreactivity was used as a marker of the preBötC. Injections were made using micropipettes (~40 µm tip), placed bilaterally into the preBötC. Injections targeted to the center of the preBötC were placed 0.15 mm caudal to the hypoglossal canal, 1.2 mm lateral to the midline, and 0.24

mm dorsal to the ventral medullary surface. Small corrections were made to avoid puncturing of blood vessels on the surface of the medulla. All injections were made using a series of pressure pulses (Picospritzer; Parker-Hannifin).

Analysis of the strength of the Breuer-Hering inflation reflex

The Breuer-Hering inflation reflex (BHIR) was triggered by inflating the lungs using constant positive air pressure (CPAP; 8 cm H_2O). The strength of the BHIR (SBHIR) was evaluated by measuring the duration of the resultant inflation-induced apnea (T_{E-INF}). CPAP was terminated after the reflex was "broken", i.e., when inspirations reappeared despite CPAP. SBHIR was calculated as $[(T_{E-INF}/T_{E-CON})-1]$, where T_{E-CON} is the expiratory duration during the control period immediately preceding CPAP (Janczewski et al., 2013).

Unit recordings

To record neuronal activity from the preBötC, mice were anesthetized and positioned supine on a stereotaxic frame. The ventral surface of the brainstem was exposed as described above, and the meninges ruptured. Melted 5-10% agar was placed on the medullary surface to prevent the movement of the brainstem. A glass electrode (~3 µm inner tip diameter) was connected to a headstage (HZP; Grass Instruments), and spike activity was recorded 0.15 mm caudal to the hypoglossal canal, 1.2 mm lateral to the midline, and 0.15-0.35 mm dorsal to the ventral medullary surface. The signal was amplified and sampled at 10 kHz (PowerLab 16SP; ADInstruments). The optic fiber was positioned adjacent to the glass electrode, in soft contact with the ventral surface 0.13-0.15 mm caudal to the hypoglossal canal and 1.2 mm lateral to the midline, ~250 µm ventral to the center of preBötC. Timed photostimulation was applied to identify neurons and determine their response to laser stimulation.

Histology

At the end of each experiment, mice were transcardially perfused with saline followed by 4% paraformaldehyde in phosphate buffer. The brains were collected, postfixed overnight at 4 ℃ and cryoprotected in 30% sucrose in PBS for 24-48 h before sectioning. 40 µm brainstem transverse sections were then cut using a cryostat (CryoStar NX70, Leica Microsystems). Serial sections were immunostained for detection of specific neuronal markers.

Immunohistochemistry was performed according to the following protocol. Free-floating sections were rinsed in PBS and incubated with 10% normal donkey antiserum (NDS) and 0.2% Triton X-100 in PBS for 60 min to reduce nonspecific staining and increase antibody penetration. Sections were incubated overnight with primary antibodies diluted in PBS containing 1% NDS and 0.2% Triton X-100. The following day, sections were washed in PBS, incubated with the

specific secondary antibodies conjugated to the fluorescent probes diluted in PBS for 2 h. Sections were further washed in PBS, mounted, and coverslipped with Fluorsave mounting medium (Millipore). The primary antibodies used for this study were as follows: rabbit polyclonal anti-somatostatin-14 (1:500; Peninsula Laboratories), mouse monoclonal anti-NeuN (1:500; Millipore; MAB377), rabbit anti-NK1R (1:500, Chemicon) and chicken polyclonal anti-GFP (1:500; Aves Labs). DyLight488 or Cy2 donkey anti-chicken, Rhodamine Red-X donkey anti-rabbit, DyLight488 donkey anti-rabbit, Cy5 donkey anti-rabbit, DyLight488 donkey anti-mouse and Cy5 donkey anti-mouse conjugated secondary antibodies (1:250; Jackson ImmunoResearch) were used to detect primary antibodies. Slides were observed under an AxioCam2 Zeiss fluorescent microscope connected with AxioVision acquisition software or under a LSM510 Zeiss confocal microscope with Zen software (Carl Zeiss). Images were acquired, exported in TIFF files, and arranged to prepare final figures in Zen software (Carl Zeiss) and Adobe Photoshop (Adobe).

Data analysis and statistics

Traces were recorded on a computer using LabChart 7 Pro (AD Instruments) and analyzed using LabChart 7 Pro (ADInstruments), Excel, and Igor Pro (Wavemetrics, Inc.) software. The absolute value of GG_{EMG} signals was digitally integrated with a time constant of 0.05 s to calculate peak amplitude. The flow signal was high-pass filtered (>0.1 Hz) to eliminate DC shifts and slow drifts, and used to calculate respiratory rate, period, inspiratory (T_I) and expiratory (T_E) durations. After filtering, the flow signal was digitally integrated to obtain tidal volume (V_T).

In photostimulation experiments, an average of 3-5 identical stimulus were applied in each mouse for each experiment. For mice using for phase resetting analysis, at least one stimulus was given in each time bin (see below). Unpaired t-tests were used to determine statistical significance of changes before and after photostimulation or pharmacological injections. For statistical comparisons of more than two groups, repeated-measures (RM) ANOVAs were performed. For one-way and two-way RM ANOVAs, post hoc significance for pairwise-comparisons was analyzed using Holm-Sidak method. The n value indicates the number of mice used for statistic analysis. Significance was set at $P<0.05$. Data are shown as mean ±SD.

Reset analysis

The photostimulation-evoked reset of the respiratory pattern was studied by applying bilateral preBötC SPP at different times throughout the respiratory cycle. The respiratory cycle duration was defined as the time between peaks of successive integrated flow. Perturbed cycle duration is the respiratory period during the light-affected cycle. The cycle immediately preceding the perturbed cycle is defined as control cycle. The times at which stimulation was delivered were

translated into phases (stimulus phase), which were calculated based on the time from the peak of the previous integrated flow to the onset of stimulus delivery, divided by the control cycle duration (Lewis et al., 1990). The stimulus phase was binned into 10 equally sized (36 °) phase bins (Witt et al., 2013). The shift in respiratory phase resulting from bilateral preBötC SPP (phase shift) was calculated as the perturbed cycle duration divided by the control cycle duration. If the stimulation had no effect, the perturbed cycle duration would equal the control cycle duration, and the phase shift value would be 1.0. If the photostimulation leads to a phase advance, the value is <1.0, and, if the photostimulation leads to a phase delay, the value is >1.0. The observed phase shifts were averaged over each bin. Phase response curves (PRCs) were then generated by plotting the phase shift versus the stimulus phase using software written in Igor Pro (Wavemetrics, Inc.).

Supplemental References

Adamantidis, A.R., Zhang, F., Aravanis, A.M., Deisseroth, K., and de Lecea, L. (2007). Neural substrates of awakening probed with optogenetic control of hypocretin neurons. Nature *450*, 420-424.

Cardin, J.A., Carlen, M., Meletis, K., Knoblich, U., Zhang, F., Deisseroth, K., Tsai, L.H., and Moore, C.I. (2009). Driving fast-spiking cells induces gamma rhythm and controls sensory responses. Nature *459*, 663-667.

Gradinaru, V., Thompson, K.R., Zhang, F., Mogri, M., Kay, K., Schneider, M.B., and Deisseroth, K. (2007). Targeting and readout strategies for fast optical neural control in vitro and in vivo. The Journal of neuroscience : the official journal of the Society for Neuroscience *27*, 14231-14238.

Lewis, J., Bachoo, M., Polosa, C., and Glass, L. (1990). The effects of superior laryngeal nerve stimulation on the respiratory rhythm: phase-resetting and aftereffects. Brain research *517*, 44-50.

Paxinos, G., and Franklin, K.B. (2003). The mouse brain in stereotaxic coordinates: compact second edition. San Diego: Academic.

Witt, A., Palmigiano, A., Neef, A., El Hady, A., Wolf, F., and Battaglia, D. (2013). Controlling the oscillation phase through precisely timed closed-loop optogenetic stimulation: a computational study. Frontiers in neural circuits *7*, 49.